JOURNAL OF AGRICULTURAL AND FOOD CHEMISTRY

Article

pubs.acs.org/JAFC

# Allicin Induces p53-Mediated Autophagy in Hep G2 Human Liver Cancer Cells

Yung-Lin Chu,[†] Chi-Tang Ho,[†,‡] Jing-Gung Chung,[§] Raghu Rajasekaran,[†] and Lee-Yan Sheen*[,†]

[†]Institute of Food Science and Technology, National Taiwan University, Taipei, Taiwan, Republic of China

[‡]Department of Food Science, Rutgers University, New Brunswick, New Jersey, United States

[§]Department of Biological Science and Technology, China Medical University, Taichung, Taiwan, Republic of China

**ABSTRACT:** Garlic has been used throughout history for both culinary and medicinal purpose. Allicin is a major component of crushed garlic. Although it is sensitive to heat and light and easily metabolized into various compounds such as diallyl disulfide, diallyl trisulfide, and diallyl sulfide, allicin is still a major bioactive compound of crushed garlic. The mortality of hepatocellular carcinoma is quite high and ranks among the top 10 cancer-related deaths in Taiwan. Although numerous studies have shown the cancer-preventive properties of garlic and its components, there is no study on the effect of allicin on the growth of human liver cancer cells. In this study, we focused on allicin-induced autophagic cell death in human liver cancer Hep G2 cells. Our results indicated that allicin induced p53-mediated autophagy and inhibited the viability of human hepatocellular carcinoma cell lines. Using Western blotting, we observed that allicin decreased the level of cytoplasmic p53, the PI3K/mTOR signaling pathway, and the level of Bcl-2 and increased the expression of AMPK/TSC2 and Beclin-1 signaling pathways in Hep G2 cells. In addition, the colocalization of LC3-II with MitoTracker-Red (labeling mitochondria), resulting in allicin-induced degradation of mitochondria, could be observed by confocal laser microscopy. In conclusion, allicin of garlic shows great potential as a novel chemopreventive agent for the prevention of liver cancer.

**KEYWORDS:** *allicin, p53, autophagy, LC3-II, Hep G2 cells*

## INTRODUCTION

Garlic [(*Allium sativum* (Liliaceae)] is an ancient spice and a medicine used for centuries around the world.[1] Garlic constituents are found to possess chemoprotective and chemopreventive properties and are effective against different types of cancers such as skin,[2] digestive,[3] prostate,[4] and lung[5] cancers. Allicin (2-propene-1-sulfinothioic acid *S*-2-propenyl ester) is a key molecule of garlic and is responsible for the pungent smell of garlic. It is released from its nonvolatile precursor alliin (*S*-allyl-L-cysteine sulfoxide) by an alliinase-mediated degradation which takes place when the garlic tissues are disrupted. Allicin is unstable and is rapidly metabolized into diallyl sulfide, diallyl disulfide, and diallyl trisulfide in vivo. Allicin has been reported to inhibit the viability and proliferation of several tumors, including colon, breast, uterine cervix, and lymph tumors, suggesting that the apoptosis could be a general mechanism of action.[6]

Liver cancer is prevalent with a high mortality rate among cancers. In Taiwan, liver cancer ranks number one in males and second in females among cancer mortality in 2010. So far the therapies of liver cancer have included surgery, chemical therapy, and target therapy, but there is no perfect treatment. An alternative therapy for liver cancer is certainly needed. There are a few studies showing that allicin could induce apoptosis in liver cancer cells[7] but no report of allicin causing autophagic cell death in liver cancer cells. In this study, we focused on allicin-induced autophagic cell death in human liver cancer Hep G2 cells.

Apoptosis is characterized by apoptotic body formation, chromatin condensation, DNA fragmentation, cell cycle arrest, endoplasmic reticulum (ER) stress, mitochondrion dysfunction, and activated caspases such as caspase-3. It is also classified as extrinsic cell death that involves caspase-8, Fas, and FasL activation, intrinsic cell death which includes mitochondrial release of cytochrome *c* and caspase-9 activation, and caspase-independent cell death involving apoptotic-inducing factor (AIF) and endonuclease G (Endo G) release from mitochondria and translocation into the nucleus.[8]

Autophagy is an intracellular lysosome degradation and a cell self-protective mechanism of nutrient starvation. Autophagy has been involved in many physiological and pathological processes and contributes to broad mammalian diseases, such as nutrient exhaustion, infection, and metabolic disease.[9] Generally, the process of autophagy is started by a preautophagosomal structure (PAS) and then formation of a double-membrane-bound autophagosome which will receive a lysosome to become an autophagolysosome and degrade by lysosomal hydrolases. Finally, the degradation products can be reused by the cell for metabolism.[10]

Mitochondrial autophagy has been classified to be part of a nonselective regulation of autophagy and selective degradation of damaged mitochondria. Damaged mitochondria may produce ROS, decrease the mitochondrion membrane potential ($\Delta\Psi$m), and release AIF, Endo G, cytochrome *c*, Bax, or other apoptotic protein to promote cell death.[11] Removal and degradation of the mitochondria with damaged components and dysfunction is presumed via autophagy.[12,13]

Received: March 27, 2012
Revised: August 3, 2012
Accepted: August 5, 2012
Published: August 6, 2012

ACS Publications © 2012 American Chemical Society

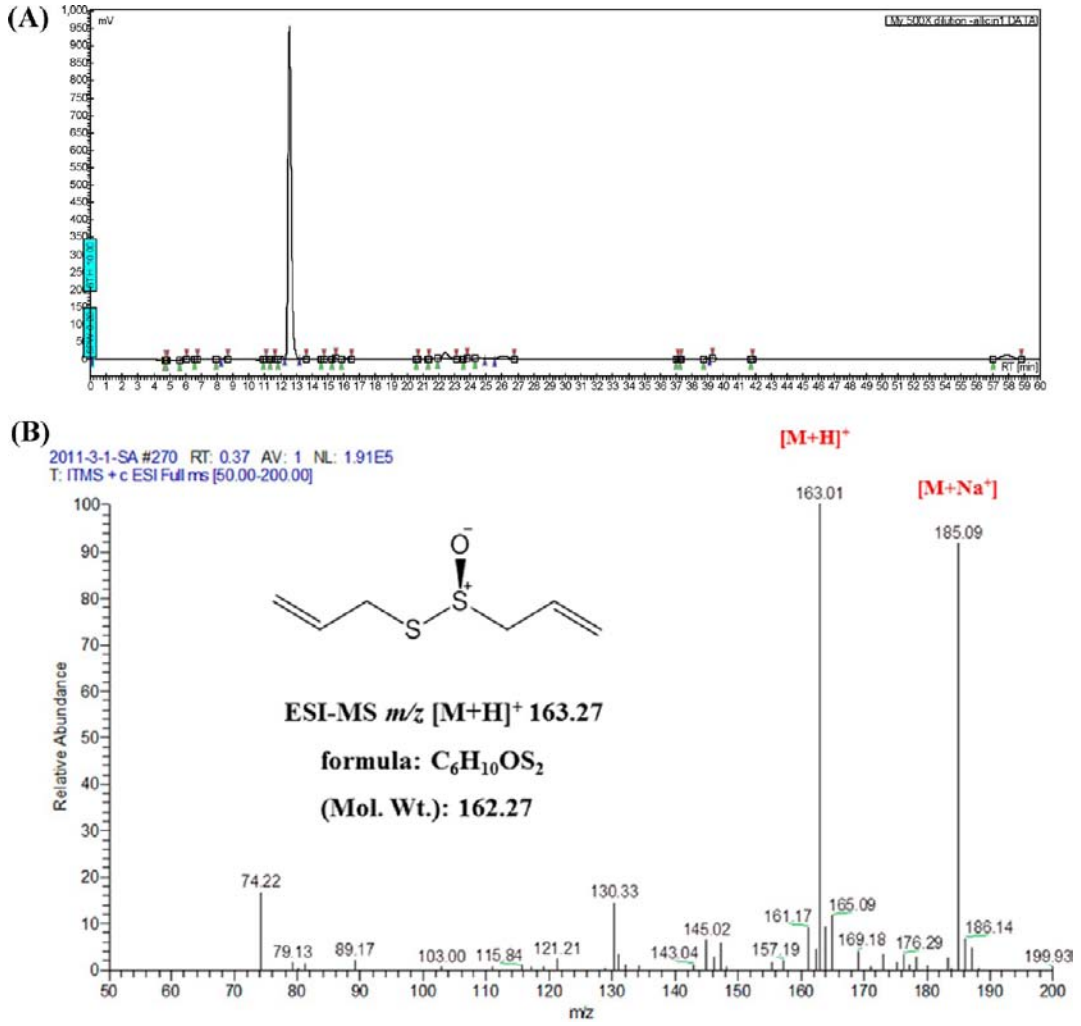


**Figure 1.** Representative chromatogram profiles of the extracted allicin. (A) High-performance chromatogram of the extracted allicin (retention time 12 min). Conditions: column, COSMOSIL 5C18-AR-II RP-C18; flow rate, 2 mL/min; detector, 254 nm; mobile phase, methanol (60%)/water (40%). (B) Extracted ion chromatogram (ESI(+)), *m*/*z* 163.01, for allicin separated in an LXQ LC/MS/MS system.

The aim of the present study is to evaluate the chemoprotective effect of allicin against human liver cancer cell line Hep G2 and to elucidate the molecular mechanisms involved thereof.

## MATERIALS AND METHODS

**Chemicals and Reagents.** Allicin standard, dimethyl sulfoxide (DMSO), potassium phosphates, phosphate-buffered saline (PBS), 3-methyladenine (3-MA), propidium iodide (PI), ribonuclease-A, Tris−HCl, Triton X-100, and trypan blue were purchased from Sigma-Aldrich Chemical Co. (St. Louis, MO). Dulbecco's modified Eagle's medium (DMEM) with 2 mM L-glutamine + 10% fetal bovine serum, penicillin−streptomycin, and trypsin−EDTA were obtained from Gibco BRL (Grand Island, NY). 2′,7′-Dichlorfluorescein-diacetate (DCFH-DA) and 3,3′-dihexyloxacarbocyanine iodide ($DiOC_6$) were obtained from Invitrogen Life Technologies. Annexin V-FITC/PI Apoptosis Detection Kit I was obtained from BD Biosciences (San Jose, CA) (FITC = fluorescein isothiocyanate). MitoTracker-Red was purchased from Invitrogen.

**Sample Preparation.** Allicin was synthesized according to a published method with slight modification.[14] Briefly, 40 mL of dichloromethane with 0.08 M diallyl disulfide (DADS) was mixed slowly with 100 mL of dichloromethane containing 17.56 g (85%, 1 equiv) of *m*-chloroperoxybenzoic acid (mCPBA). After the mixture was stirred for 1 h, the pH was adjusted to 7.0 with 10% sodium carbonate, and the organic phase was washed twice with 150 mL of deionized distilled $H_2O$. Anhydrous magnesium sulfate was mixed with the solvent and the resulting mixture filtered through a 0.45 μm membrane for dehydration. All the above steps were performed at 0−4 °C. The solvent was removed from the sample using a rotary evaporator, and the crude allicin was obtained. This crude allicin was further purified by column chromatography and eluted with a solvent mixture of tetrahydrofuan (THF)/*n*-hexane (1:10), and the solvents were again removed using a rotary evaporator at the room temperature of 25 °C to obtain 9.78 g of allicin (70% yield). The HPLC mobile phase consisted of methanol (60%)/deionized distilled $H_2O$ (40%) at a flow rate of 2 mL/min, and its absorbance was detected at 254 nm. Since the retention time of standard allicin was 12−13 min in 60% methanol conditions, pure allicin eluates were obtained by collection from 12 to 13 min in every injection of the synthesized allicin and pooled together (Figure 1). Quantitative analysis of allicin was performed using an LC-NET II/ADC Jasco system equipped with a chromatography station for Jasco-Chrompass software. To get a higher purity of allicin, the 70% allicin was separated on a semipreparative RP-HPLC column (Cosmosil $5C_{18}$-AR-II, 5 μm, 250 mm ×10 mm i.d.; Nacalai Tesque, Tokyo, Japan). The allicin purity was over 95% as determined by HPLC/UV analysis.[15] This was used to treat the Hep G2 cells.

**Mass Spectrometry.** Qualitative analysis was performed with an LXQ LC/MS/MS Advantage ion trap mass spectrometer (Thermo Finnigan, San Jose, CA). The MS detector was optimized by injecting a 10 μL/min flow speed of allicin standard (0.1 mg/mL in methanol)

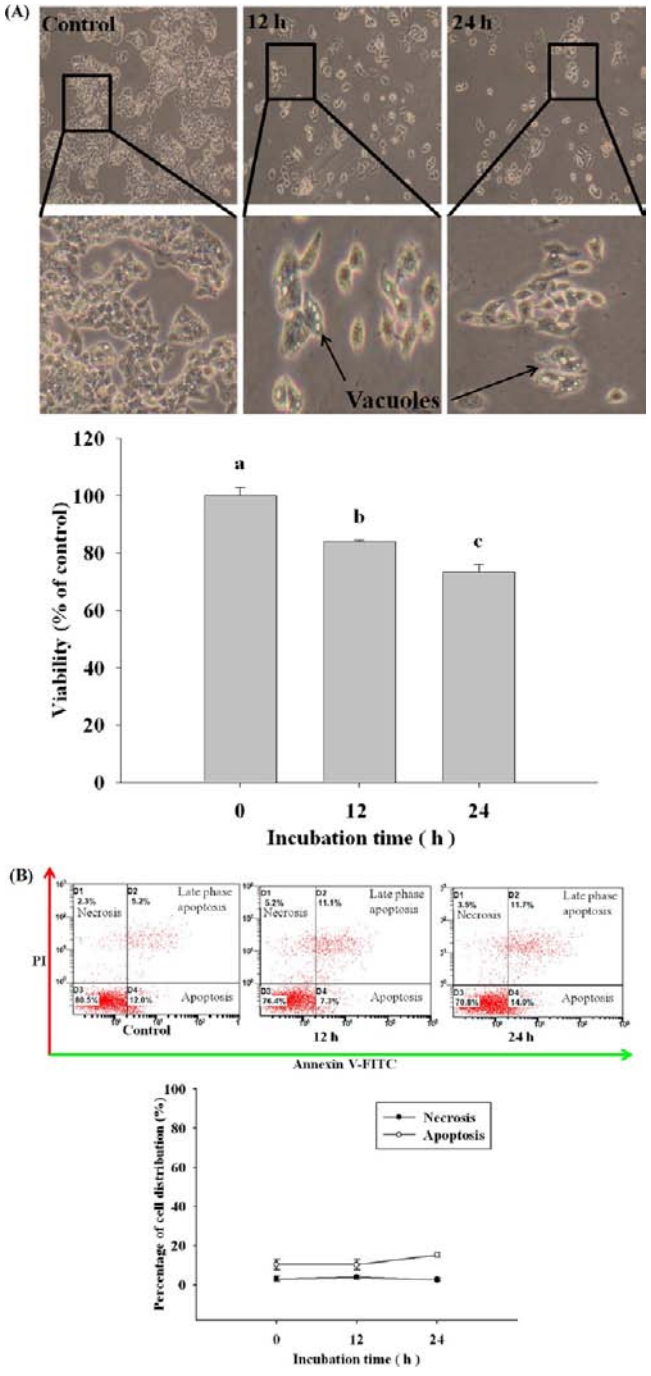


**Figure 2.** Effect of allicin on cell morphology and percentage of viable cells in Hep G2 human liver cancer cells. (A) Vacuoles of the cells were examined and photographed by phase-contrast microscopy and the viability of Hep G2 cells determined. Cells were cultured in 35 $\mu$M allicin for 12 and 24 h. (B) Percentage of apoptotic and necrotic cell induction by allicin-treated Hep G2 cells. Cells were exposed to 35 $\mu$M allicin for 12 and 24 h, and the distributions of apoptosis (lower right panel) and necrosis (upper left panel) were assessed by annexin V–FITC/PI assay. All results are reported as means ± SD, and the differences between the allicin-treated and control groups were analyzed by one-way ANOVA and Duncan's multiple comparison tests (SAS Institute Inc., Cary, NC) to determine significant differences among treatments, $p < 0.05$.

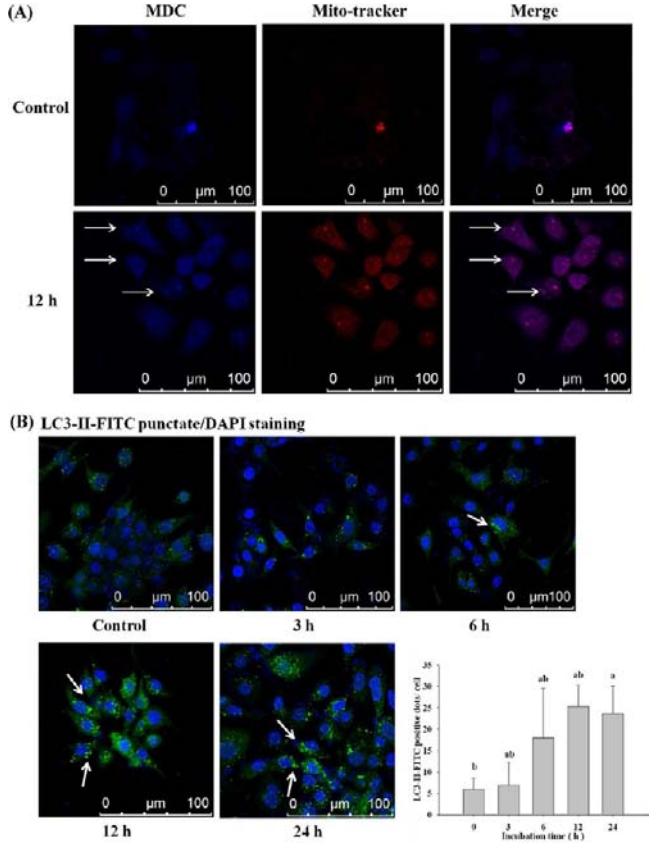


**Figure 3.** Allicin induced formation of autophagic vacuoles and autophagosomes in Hep G2 human liver cancer cells. Cells were exposed to 35 $\mu$M allicin for varying duration. (A) The autophagosome staining was measured by MDC labeling in Hep G2 cells. MDC, an autofluorescent drug, accumulates in autophagosomes and stains autophagic vacuoles in live cells. (B) Quantization of autophagosome formation was analyzed by LC3-II–FITC punctate after allicin treatment in Hep G2 cells. Arrows indicate the formation of autophagosomes in allicin-treated cells. Scale bars as presented.

and the synthesized allicin to obtain the maximum intensities of $[M + H]^+$ ions. The parameters optimized in the positive ion mode were as follows: sheath gas ($N_2$) flow rate, 6 arbitrary units; auxiliary gas ($N_2$) flow rate, 8 arbitrary units; sweep gas flow rate, 0 arbitrary units; ion spray voltage, 6.0 kV; capillary temperature, 210 °C; capillary voltage, 3 V; tube lens offset voltage, 25 V. For full-scan MS analysis, the spectral range of $m/z$ 10–200 was recorded. In full-scan MS, a data-dependent acquisition was set so that the two most abundant ions would trigger tandem mass spectrometry ($MS^n$, $n$ = 2–4). The isolation width of the precursor ions was 3.0 $m/z$, and the collision energy for $MS^n$ was adjusted to 35% in LC/MS analysis.[16]

**Cell Culture.** The human liver carcinoma Hep G2 ($p53^{wild\ type}$) cell lines were obtained from the Department of Medical Research and Education, Taipei Veterans General Hospital, Taipei, Taiwan. Hep G2 cells were cultured in a 10 $cm^2$ dish with DMEM (Gibco BRL). The cell medium with 2 mM L-glutamine was adjusted to contain 10% fetal bovine serum (Gibco BRL) and 1% penicillin–streptomycin (100 U/mL penicillin and 100 $\mu$g/mL streptomycin) and grown at 37 °C under a humidified 5% $CO_2$ atmosphere. Adherent cells were suspended by 1 mL of trypsin–EDTA for 5 min at 37 °C.

**Determination of the Cell Morphology and Viability and Examination of the Cell Vacuoles.** Liver cancer cells were seeded at a concentration of $1 \times 10^5$ cells/well in a 12-well plate for 24 h and then incubated with various concentrations of allicin at 37 °C, 5% $CO_2$, and 95% air for 24 h. The vacuoles of the cells were examined and photographed by phase-contrast microscopy for the examination of morphological changes.[17] Then the cells were harvested by centrifugation, stained with PI (5 $\mu$g/mL), and analyzed by flow cytometry (Becton-Dickinson, San Jose, CA) for viability measurements


dx.doi.org/10.1021/jf301298y | J. Agric. Food Chem. 2012, 60, 8363–8371

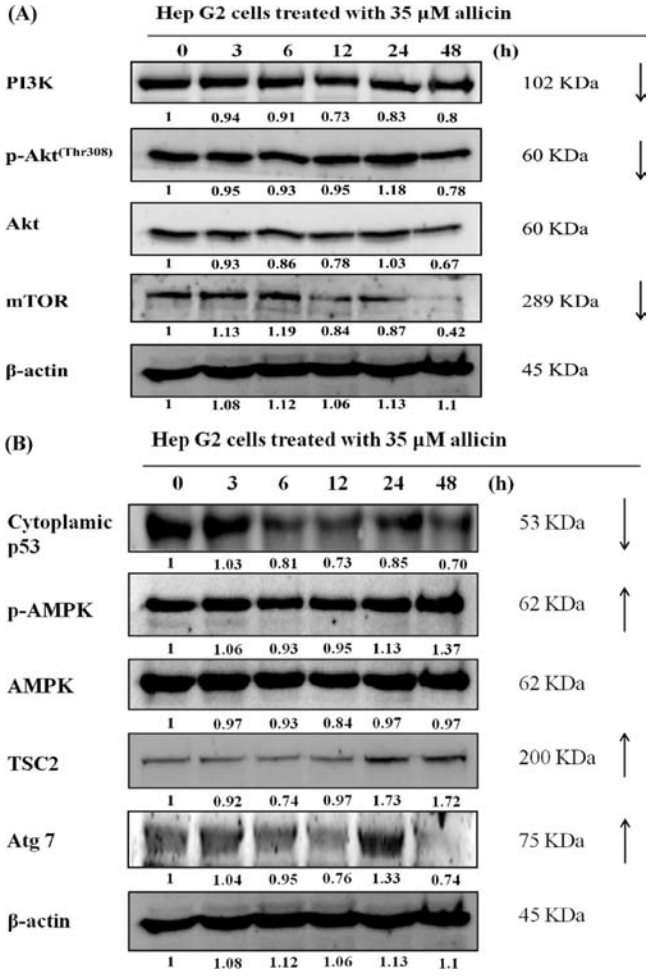


**Figure 4.** Representative immunoblots depicting changes in the expression levels of proteins associated with autophagic cell death in Hep G2 cells cocultured with allicin at 35 $\mu$M for 0, 3, 6, 12, 24, and 48 h. The protein expressions of (A) PI3K, AKT, and mTOR and (B) cytoplamic p53, AMPK, Atg7, and TSC2 were quantified by densitometry on the immunoblots by Image J software as described in the Materials and Methods.

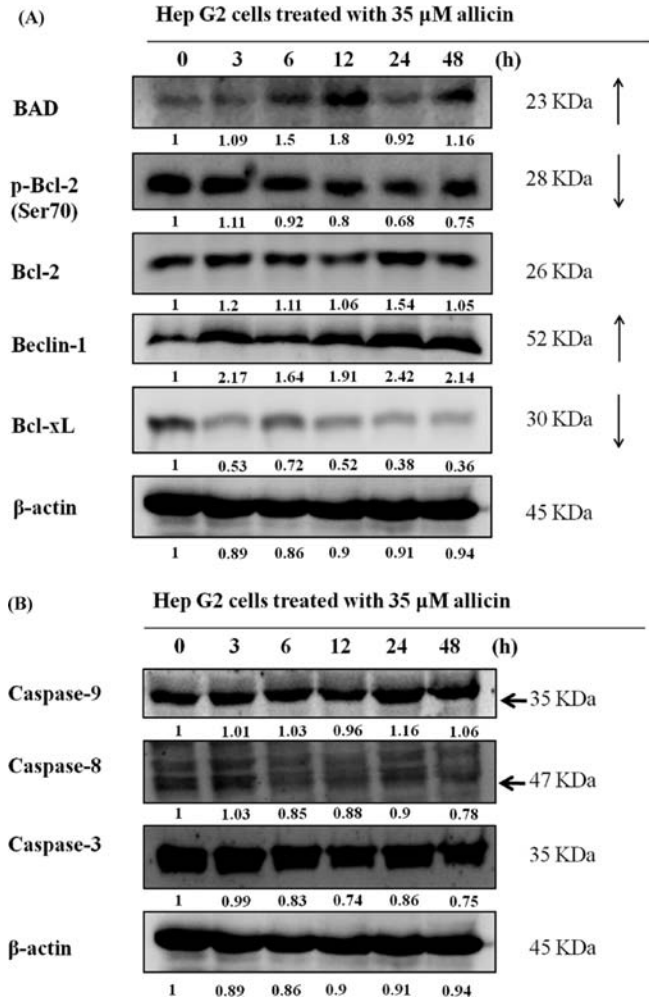


**Figure 5.** Immunoblotting of mitochondrion-related autophagy and apoptotic proteins in Hep G2 cells after treatment with 35 $\mu$M allicin. The protein expressions of (A) BAD, Bcl-2, Beclin-1, and Bcl-xL and (B) caspase-3, -8, and -9 were quantified on the blots using Image J software by densitometry as described in the Materials and Methods.

as a PI exclusion assay.[18] The cells that were treated with 0.1% DMSO were used as a control of 100% survival.[18]

**Detection of the Mitochondrial Membrane Potential ($\Delta\Psi$m).** Approximately $1 \times 10^5$ liver cancer cells/mL were treated with 35 $\mu$M allicin for 0.5, 1, 3, 6, and 12 h, and then cells from each treatment were resuspended in 500 $\mu$L of $DiOC_6$ (4 $\mu$mol/L) for $\Delta\Psi$m determination. Cells were incubated at 37 °C for 30 min before being analyzed by flow cytometry.

**Annexin V–FITC/PI Double Staining Assay.** To analyze allicin-induced apoptosis of liver cancer cells, we seeded cells at a concentration of $1 \times 10^5$ cells/well in a 12-well plate. The Hep G2 cells were treated with 35 $\mu$M allicin for 0, 3, 6, 12, and 24 h and then washed twice with PBS. Next we resuspended the cells in 1× binding buffer with $1 \times 10^6$ cells/mL and transferred 100 $\mu$L of 1× binding buffer with $1 \times 10^5$ cells/mL to a 5 mL flourescence activated cell sorting (FACS) tube. The following step was performed in the dark: 5 $\mu$L of annexin V–FITC and 10 $\mu$L of PI were added. In the end, we added 400 $\mu$L of 1× binding buffer to the sample tube with analysis by flow cytometry within 1 h.[19]

**Western Blot Analysis.** Liver cancer cells ($1 \times 10^7$ cells) seeded in a 10 $cm^2$ dish were treated with 35 $\mu$M allicin for 0, 3, 6, 12, 24, and 48 h. The cells were harvested and lysed with lysis buffer containing 40 mM Tris–HCl (pH 7.4), 10 mM EDTA, 120 mM NaCl, 1 mM dithiothreitol, and 0.1% nonide P-40, and the protein concentrations of the cell lysate and subcellular fraction were quantitated with a protein assay kit (Bio-Rad Laboratories, Hercules, CA). The total proteins (26 $\mu$g) were used for Western blot analysis, and all samples were subjected to 10% sodium dodecyl sulfate–polyacrylamide gel electrophoresis (SDS–PAGE) for 60 min. Then the proteins were transferred to poly(vinylidene fluoride) (PVDF) membranes (Millipore, Billerica, MA) and incubated with primary antibodies such as (A) mTOR, TSC2, and Beclin-1 (Genetex, Irvine, CA) and (B) p53, Bcl-2, Bcl-xL, Bax, caspase-9, caspase-3, and caspase-8 (Cell Signaling Technology, Danvers, MA), washed, and incubated with horseradish peroxidase (HRP)-conjugated secondary antibody for detection by a WesternBreeze chemiluminescent kit (Invitrogen) according to the manufacturer's instructions. As an internal control, we used anti-$\beta$-actin (a rabbit monoclonal antibody).[20]

**Confocal Laser Scanning Microscopy for LC3-II–FITC Punctate Formation.** Liver cancer cells at a density of $5 \times 10^4$ cells/well were cultured on Polysine microscope adhesion slides (Cel-line, Thermo) and then treated with or without 35 $\mu$M allicin for 24 h. Then the cells on the slides were fixed in 4% paraformaldehyde in PBS for 15 min and permeabilized with 0.1% Triton-X 100 in PBS for 0.5 h with blocking of nonspecific binding sites using 2% BSA as described previously. Primary antibodies to LC3-II (1:3000 dilution) (green fluorescence) were used to stain the fixed cells overnight, and then the cells were washed twice with PBS and stained with secondary antibody (FITC-conjugated goat antirabbit immunoglobulin G (IgG) at 1:100 dilution),

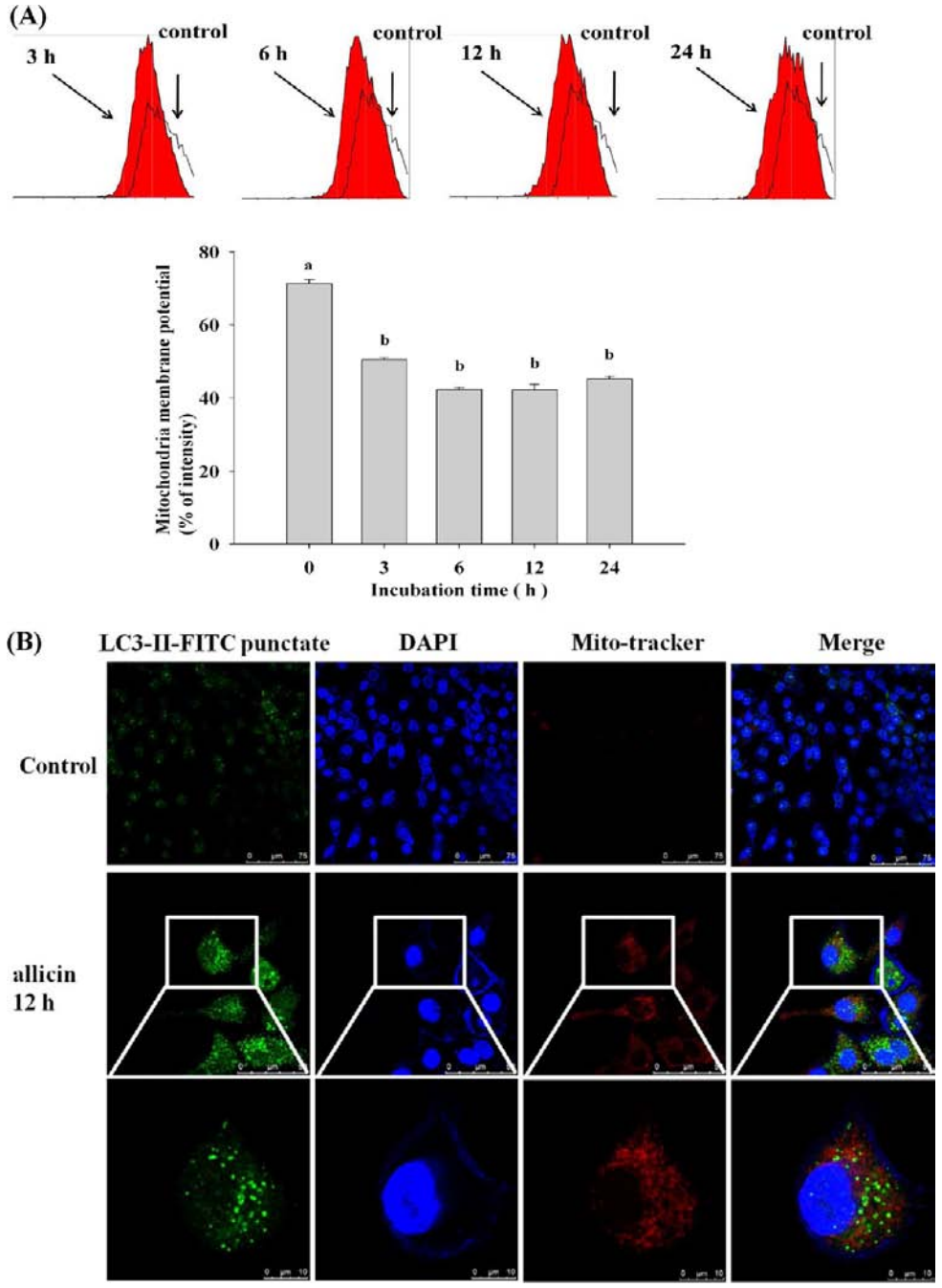


**Figure 6.** Allicin (35 $\mu$M) induced the depolarization of mitochondrial membrane and caused autophagosomes to engulf the mitochondria in Hep G2 cells. (A) Allicin decreased the level of $\Delta\Psi$m and damaged the mitochondria. (B) Colocalization of autophagosomes labeled with LC3-II−FITC and mitochondria labeled with MitoTracker-Red dye. Scale bars as presented.

followed by DNA staining with 4′,6-diamidino-2-phenylindole (DAPI; blue fluorescence) as described previously. All samples were visualized using a Leica TCS SP5 II confocal spectral microscope. All image data were quantified by Image J software, which is an image-inspired Java program from the National Institutes of Health (NIH).[21]

**Analysis of Colocalization of LC3-II−FITC Punctate and MitoTracker-Red Labeling.** Hep G2 cells were seeded on Polysine slides and treated with 35 $\mu$M allicin for various durations. Confocal images of immunostaining against LC3-II (1:3000 dilution) and 500 nM MitoTracker-Red and DAPI staining were acquired using a Leica TCS SP5II confocal laser scanning microscope. LC3-II- and MitoTracker-Red-positive dots per cell were analyzed using Image J software.[22]

**Labeling of Autophagic Vacuoles with Monodansylcadaverine (MDC).** Hep G2 cells were seeded on Polysine slides and treated with 35 $\mu$M allicin for 12 h. After allicin treatment, the Hep G2 cells were incubated for 15 min with 50 $\mu$M MDC at 37 °C and 500 nM MitoTracker-Red in live cells and then fixed immediately. Because the autofluorescence of MDC bleaches quickly, fixed Hep G2 cells must be analyzed within 2 days of fixing. MDC is an autofluorescent drug which accumulates in autophagolysosomes to measure the autophagic process.[23] All process steps were operated in the dark.

**Statistical Analysis.** All results are reported as the mean ± SD, and the difference between the allicin-treated and control groups was analyzed by one-way analysis of variance (ANOVA) and Duncan's multiple comparison tests (SAS Institute Inc., Cary, NC) to determine significant differences among treatments, $p < 0.05$.

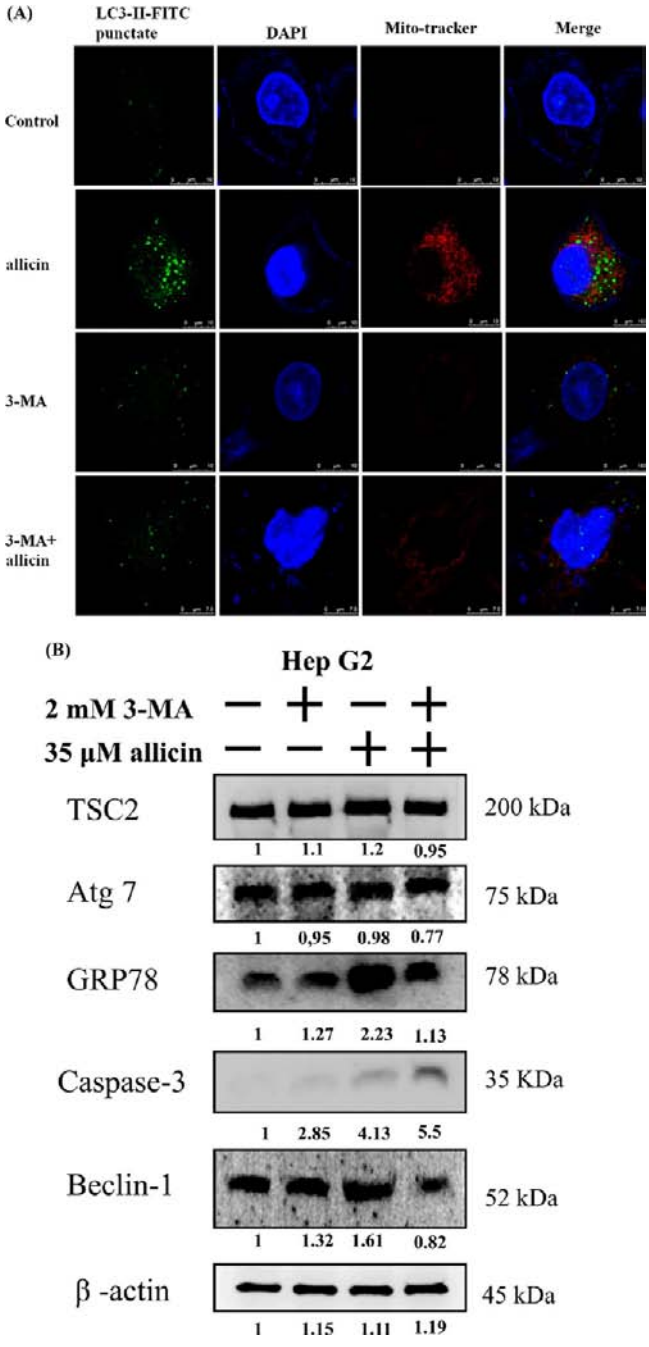


**Figure 7.** 3-MA inhibited allicin-induced autophagy in Hep G2 cells but triggered apoptosis. Cells were pretreated with 2.0 mM 3-MA for 2 h and with 35 $\mu$M allicin for 12 h and studied using confocal microscopy. (A) We stained autophagosomes with LC3-II−FITC and labeled mitochondria with MitoTracker-Red. Scale bars as presented. (B) 3-MA (autophagy inhibitor) pretreatment for 24 h suppressed protein expression of Atg7, TSC2, GRP78, and Beclin-1 induced by allicin, similar to the results of pharmacological inhibition, but activated caspase-3.

## RESULTS

**HPLC and HPLC/MS/MS Chromatograph of Synthesized Allicin.** To investigate the purity of synthesized allicin, the elution time was set at 12−13 min in 60% methanol conditions, and a 95% purity was examined with an HPLC/UV system (Figure 1A). Furthermore, the extracted ion chromatogram of (ESI(+), $m/z$ 163.01 and 185, for synthesized allicin was confirmed by MS spectrometry (Figure 1B).

**Effects of the Viability of HepG2 Cells after 12 and 24 h and Distribution of Apoptosis and Necrosis.** To determine the effect of allicin on the morphology of Hep G2 cells, the vacuoles of the cells were examined with a phase-contrast microscope. The viability of liver cancer cells was measured by a flow cytometric assay (Figure 2A). Allicin treatment at 35 $\mu$M decreased the viability of Hep G2 cells after 12 and 24 h significantly. However, annexin V−FITC/PI data indicated that the allicin has no apoptosis and necrosis effect on Hep G2 cells after 12 and 24 h (Figure 2B).

**Allicin Induces Autophagolysosome Formation in Hep G2 Cells.** Figure 3A shows that allicin increased the fluorescence expression of MDC, which labeled autophagolysosomes in Hep G2 cells. In addition, allicin treatment of Hep G2 cells increased the LC3-II−FITC punctate formation in a time-dependent manner (Figure 3B). The results indicated that allicin induced autophagy and increased the formation of autophagosomes and autophagolysosomes in Hep G2 cells.

**Effect of Allicin on Autophagy and Apoptosis-Associated Protein Levels in Hep G2 ($p53^{wild\ type}$) Cells.** Figures 4 and 5 show that allicin increased the levels of Beclin-1, Bad, p-AMPK, TSC2, and Atg7 but decreased the levels of PI3K/mTOR, p-Bcl-2, Bcl-xL, and cytoplasmic p53 in Hep G2 cells. In Figure 4, our studies demonstrated that allicin induced p53-mediated autophagic cell death in liver cancer cells through activation of p-AMPK and TSC2 signaling pathways and inhibition of mTOR (mammalian target of rapamycin) and cytoplasmic p53 signaling pathways. Figure 5B shows that allicin did not activate protein expressions of caspase-3, -8, and -9 in Hep G2 cells and induced caspase-dependent apoptotic cell death.

**Allicin Affects Mitochondrial Depolarization and the Mitochondrial Membrane Potential ($\Delta\Psi$m).** To investigate whether allicin-caused cell death was through the mitochondrial death pathway, liver cancer cells were treated with 35 $\mu$M allicin for different durations and the level of mitochondrial membrane potential was measured by flow cytometry (Figure 6A). The results showed that allicin treatment caused a decrease of $\Delta\Psi$m of Hep G2 cells and degradation of mitochondria (Figure 6B).

**Allicin Induced Degradation of Mitochondrial Autophagy and Blocked Protein Induction by Allicin Treatment in Hep G2 Cells.** To further investigate the type of autophagy induction of allicin, the colocalization of autophagosomes and mitochondria was examined by LC3-II−FITC punctate formation and MitoTracker-Red labeling. The results indicated that allicin increased the autophagosomes with LC3-II−FITC punctate formation and colocalized with mitochondria (Figure 6B). Furthermore, pretreatment with 3-MA could inhibit the formation of LC3-II−FITC punctate but also block the colocalization of autophagosomes and mitochondria (Figure 7A). 3-MA inhibited the allicin-induced protein expression of TSC2, Atg7, Beclin-1, and GRP78 (Figure 7B) but activated caspase-3. All data showed that allicin induced multiple potential strategies by regulating autophagy in Hep G2 liver cancer cells.

## DISCUSSION

Allicin is a key bioactive component of fresh garlic. Numerous reports of allicin inducing apoptosis in various cancer cells are available.[6,7,24−27] From a comparison of the morphologies and cell viabilities of Hep G2 cells treated with allicin for 12 and 24 h, it could be inferred that the allicin-induced cell death and morphology changes of Hep G2 cells were not due to the phenomena of apoptosis (lower right panel) and necrosis

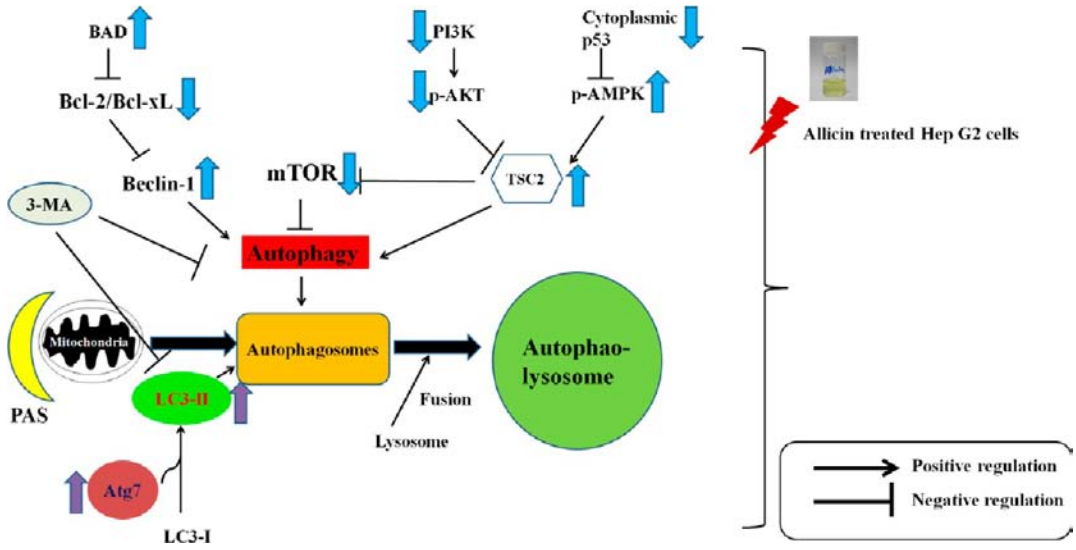


**Figure 8.** Proposed mechanism of allicin-induced autophagy in Hep G2 human liver cancer cells. Our study shows a novel mechanism of allicin-induced autophagic cell death of Hep G2 human liver cancer cells and induction of autophagy via multiple p53/AMPK, LC3-II, mTOR, and Beclin-1 signaling pathways.

(upper left panel) as evidenced by the annexin V−FITC/PI assay (Figure 2). In this study we employed human hepatocarcinoma cells to elucidate the mechanism of allicin against cancer, and this is the first study to demonstrate that allicin could induce p53-mediated autophagic cell death.

p53, a key molecule in DNA damage repair and a tumor suppressor protein, is involved in a multitude of biological processes, including autophagy, apoptosis, necrosis, cell cycle arrest, and metabolism.[28] Approximately 50% of human cancers exhibit p53 mutation.[29] Recently, p53 has been proved to be a powerful regulator of autophagy and to regulate the Warburg effect (the unusually high rate of glycolysis under aerobic conditions) that is prevalent in many cancers. Furthermore, p53 engages cellular autophagy in various pathways which include nutrient sensing pathways with proteins of famous function resulting in modulation of mTOR, AMPK, and TSC2. However, an increase in the cytoplasmic p53 inhibits the induction of autophagy, whereas an increase in the nuclear p53 induces autophagy in cancer, and the function has also been reported for tumor-derived mutants of p53.[28,30]

AMP-activated protein kinase (AMPK) is a major energy sensor and controls cellular metabolism and energy homeostasis, which could promote autophagy by phosphorylation.[31] Furthermore, AMPK directly phosphorylates TSC2 (the AMPK substrate tuberous sclerosis complex 2) and enhances its activity. TSC2 is phosphorylated by ATP depletion, which not only inhibits the mTOR pathway of protein synthesis, cell viability, and cellular energy level but also could protect cells from glucose deprivation-induced apoptosis.[32] Bcl-2 and Bcl-xL are members of the Bcl-2 family of proteins which are prominent antiautophagy proteins that suppress autophagy by binding to the protein Beclin-1, which is needed for the formation of autophagosomes in autophagy.[33]

As evident in Figures 4 and 5, allicin inhibited the cytoplasmic p53, Bcl-2/Bcl-xL, Beclin-1, and mTOR and activated the Atg7, AMPK, and TSC2 proteins. More importantly, allicin increased the protein level of LC3-II, which is the major marker associated with the inner and outer limiting membranes of autophagosomes[34] by triggering autophagy in Hep G2 cells (Figure 3B).

Some studies demonstrated that cell death could be associated with the combined system of autophagy and degradation of mitochondria.[35] It was also shown that although autophagy is initiated to recycle cell life, autophagy machinery may destroy organelles and components which are the foundations of the cell, resulting in cell death.[36] However, autophagy plays a fundamental role in controlling the life of the cell. Reports of colocalization of LC3-II−FITC punctate (biomarker of autophagy) and MitoTracker-Red dye (mitochondrion tracker) by confocal microscopy indicate autophagosomes engulf the injured mitochondria. Our findings are in agreement with these reports.[13] In the present study, allicin treatment of Hep G2 human liver cancer cells induced LC3-II−FITC punctate and colocalization with mitochondria. In addition, Atg7, TSC2, and Beclin-1 gave results similar to those of pharmacological inhibition, and the colocalization of LC3-II−FITC punctate and mitochondria induced by allicin was suppressed by 3-MA (autophagy inhibitor) pretreatment (Figure 7A), which confirms the induction of autophagy by allicin in Hep G2 human liver cancer cells. More interesting, allicin induced autophagy blocked by 3-MA but triggered apoptosis in Hep G2 cells. Some studies indicated that blocking autophagy but triggering apoptosis is also a strategy for killing cancer cells.[37] Our results demonstrated that allicin has multiple potential strategies for treating cancer by managing autophagy (Figure 7B).

In conclusion, our study reveals a novel mechanism of allicin-induced autophagic cell death of Hep G2 human liver cancer cells and induction of autophagy via multiple p53, mTOR, and AMPK signaling pathways. A proposed mechanism of allicin-induced autophagy is presented in Figure 8. Our results highlight that allicin is a novel molecular agent of p53-mediated autophagic cell death and has the potential to be used as a new complementary chemopreventive compound in liver cancer therapy.

## AUTHOR INFORMATION

### Corresponding Author

*Phone: 886-2-33664129. Fax: 886-2-23620849. E-mail: lysheen@ntu.edu.tw.

## Funding

This work was supported by the Joint Center for Instruments and Researches, College of Bioresources and Agriculture, National Taiwan University.

## Notes

The authors declare no competing financial interest.

## ■ ABBREVIATIONS

DAS, diallyl sulfide; DADS, diallyl disulfide; DATS, diallyl trisulfide; ER, endoplasmic reticulum; ROS, reactive oxygen species; $\Delta\Psi$m, mitochondrial membrane potential; 3-MA, 3-methyladenine (autophagy inhibitor); AIF, apoptotic-inducing factor; Endo G, endonuclease G; Fas receptor, CD95, death receptor; FasL, Fas ligand; LC3, MAP-1, microtubule-associated protein 1 light chain 3; PAS, preautophagosomal structure; mTOR, mammalian target of rapamycin; Atg, autophagy-related gene; Bax, Bcl-2-associated X protein; Bcl-2, B-cell lymphoma 2; AMPK, adenosine monophosphate responsive protein kinase; TSC2, target to phosphorylate tuberous sclerosis 2; PI, propidium iodide; mCPBA, *m*-chloroperoxybenzoic acid; FBS, fetal bovine serum; DMSO, dimethyl sulfoxide; PBS, phosphate-buffered saline

## ■ REFERENCES

(1) Kubec, R.; Cody, R. B.; Dane, A. J.; Musah, R. A.; Schraml, J.; Vattekkatte, A.; Block, E. Applications of direct analysis in real time-mass spectrometry (DART-MS) in *Allium* chemistry. (*Z*)-Butanethial *S*-oxide and 1-butenyl thiosulfinates and their *S*-(*E*)-1-butenylcysteine *S*-oxide precursor from *Allium siculum*. *J. Agric. Food Chem.* **2010**, *58*, 1121−1128.

(2) Wang, H. C.; Yang, J. H.; Hsieh, S. C.; Sheen, L. Y. Allyl sulfides inhibit cell growth of skin cancer cells through induction of DNA damage mediated G2/M arrest and apoptosis. *J. Agric. Food Chem.* **2010**, *58*, 7096−7103.

(3) Rajasekaran, R.; Lu, K. H.; Sheen, L. Y. Recent research progress on garlic as a potential anticarcinogenic agent against major digestive cancers. *J. Tradit. Complementary Med.* **2012**, *2*, 192−201.

(4) Liu, Z.; Li, M.; Chen, K.; Yang, J.; Chen, R.; Wang, T.; Liu, J.; Yang, W.; Ye, Z. S-allylcysteine induces cell cycle arrest and apoptosis in androgen-independent human prostate cancer cells. *Mol. Med. Rep.* **2012**, *5*, 439−443.

(5) Tang, F. Y.; Chiang, E. P.; Pai, M. H. Consumption of *S*-allylcysteine inhibits the growth of human non-small-cell lung carcinoma in a mouse xenograft model. *J. Agric. Food Chem.* **2010**, *58*, 11156−11164.

(6) Milner, J. A. A historical perspective on garlic and cancer. *J. Nutr.* **2001**, *131*, 1027S−1031S.

(7) Zhang, Z. M.; Zhong, N.; Gao, H. Q.; Zhang, S. Z.; Wei, Y.; Xin, H.; Mei, X.; Hou, H. S.; Lin, X. Y.; Shi, Q. Inducing apoptosis and upregulation of Bax and Fas ligand expression by allicin in hepatocellular carcinoma in Balb/c nude mice. *Chin. Med. J.* **2006**, *119*, 422−425.

(8) Ishitsuka, K.; Hideshima, T.; Hamasaki, M.; Raje, N.; Kumar, S.; Podar, K.; Le Gouill, S.; Shiraishi, N.; Yasui, H.; Roccaro, A. M.; Tai, Y. Z.; Chauhan, D.; Fram, R.; Tamura, K.; Jain, J.; Anderson, K. C. Novel inosine monophosphate dehydrogenase inhibitor VX-944 induces apoptosis in multiple myeloma cells primarily via caspase-independent AIF/Endo G pathway. *Oncogene* **2005**, *24*, 5888−5896.

(9) Mizushima, N.; Levine, B.; Cuervo, A. M.; Klionsky, D. J. Autophagy fights disease through cellular self-digestion. *Nature* **2008**, *451*, 1069−1075.

(10) Mizushima, N.; Yoshimori, T.; Levine, B. Methods in mammalian autophagy research. *Cell* **2010**, *140*, 313−326.

(11) Zhu, J.; Dagda, R. K.; Chu, C. T. Monitoring mitophagy in neuronal cell cultures. *Methods Mol. Biol.* **2011**, *793*, 325−339.

(12) Pavlides, S.; Vera, I.; Gandara, R.; Sneddon, S.; Pestell, R. G.; Mercier, I.; Martinez-Outschoorn, U. E.; Whitaker-Menezes, D.; Howell, A.; Sotgia, F.; Lisanti, M. P. Warburg meets autophagy: cancer-associated fibroblasts accelerate tumor growth and metastasis via oxidative distress, mitophagy, and aerobic glycolysis. *Antioxid. Redox Signaling* **2012**, *16*, 1264−1284.

(13) Wang, S. H.; Martin, S. M.; Harris, P. S.; Knudson, C. M. Caspase inhibition blocks cell death and enhances mitophagy but fails to promote T-cell lymphoma. *PLoS One* **2011**, *6*, e19786.

(14) Apitz-Castro, R.; Escalante, J.; Vargas, R.; Jain, M. K. Ajoene, the antiplatelet principle of garlic, synergistically potentiates the antiaggregatory action of prostacyclin, forskolin, indomethacin and dypiridamole on human platelets. *Thromb. Res.* **1986**, *42*, 303−311.

(15) Jansen, H.; Muller, B.; Knobloch, K. Allicin characterization and its determination by HPLC. *Planta Med.* **1987**, *53*, 559−562.

(16) Zhou, J.; Yao, S.; Qian, R.; Xu, Z.; Wei, Y.; Guo, Y. Observation of allicin-cysteine complex by reactive desorption electrospray ionization mass spectrometry for garlic. *Rapid Commun. Mass Spectrom.* **2008**, *22*, 3334−3337.

(17) Ling, Y. H.; Aracil, M.; Zou, Y.; Yuan, Z.; Lu, B.; Jimeno, J.; Cuervo, A. M.; Perez-Soler, R. PM02734 (elisidepsin) induces caspase-independent cell death associated with features of autophagy, inhibition of the Akt/mTOR signaling pathway, and activation of death-associated protein kinase. *Clin. Cancer Res.* **2011**, *17*, 5353−5366.

(18) Lu, C. C.; Yang, J. S.; Huang, A. C.; Hsia, T. C.; Chou, S. T.; Kuo, C. L.; Lu, H. F.; Lee, T. H.; Wood, W. G.; Chung, J. G. Chrysophanol induces necrosis through the production of ROS and alteration of ATP levels in J5 human liver cancer cells. *Mol. Nutr. Food Res.* **2010**, *54*, 967−976.

(19) Li, L.; Han, W.; Gu, Y.; Qiu, S.; Lu, Q.; Jin, J.; Luo, J.; Hu, X. Honokiol induces a necrotic cell death through the mitochondrial permeability transition pore. *Cancer Res.* **2007**, *67*, 4894−4903.

(20) Chung, J. G.; Yeh, K. T.; Wu, S. L.; Hsu, N. Y.; Chen, G. W.; Yeh, Y. W.; Ho, H. C. Novel transmembrane GTPase of non-small cell lung cancer identified by mRNA differential display. *Cancer Res.* **2001**, *61*, 8873−8879.

(21) Bryant, H. E.; Schultz, N.; Thomas, H. D.; Parker, K. M.; Flower, D.; Lopez, E.; Kyle, S.; Meuth, M.; Curtin, N. J.; Helleday, T. Specific killing of BRCA2-deficient tumours with inhibitors of poly(ADP-ribose) polymerase. *Nature* **2005**, *434*, 913−917.

(22) Grishchuk, Y.; Ginet, V.; Truttmann, A. C.; Clarke, P. G.; Puyal, J. Beclin 1-independent autophagy contributes to apoptosis in cortical neurons. *Autophagy* **2011**, *7*, 1115−1131.

(23) Takeuchi, H.; Kondo, Y.; Fujiwara, K.; Kanzawa, T.; Aoki, H.; Mills, G. B.; Kondo, S. Synergistic augmentation of rapamycin-induced autophagy in malignant glioma cells by phosphatidylinositol 3-kinase/protein kinase B inhibitors. *Cancer Res.* **2005**, *65*, 3336−3346.

(24) Oommen, S.; Anto, R. J.; Srinivas, G.; Karunagaran, D. Allicin (from garlic) induces caspase-mediated apoptosis in cancer cells. *Eur. J. Pharmacol.* **2004**, *485*, 97−103.

(25) Hirsch, K.; Danilenko, M.; Giat, J.; Miron, T.; Rabinkov, A.; Wilchek, M.; Mirelman, D.; Levy, J.; Sharoni, Y. Effect of purified allicin, the major ingredient of freshly crushed garlic, on cancer cell proliferation. *Nutr. Cancer* **2000**, *38*, 245−254.

(26) Zhang, W.; Ha, M.; Gong, Y.; Xu, Y.; Dong, N.; Yuan, Y. Allicin induces apoptosis in gastric cancer cells through activation of both extrinsic and intrinsic pathways. *Oncol. Rep.* **2010**, *24*, 1585−1592.

(27) Bat-Chen, W.; Golan, T.; Peri, I.; Ludmer, Z.; Schwartz, B. Allicin purified from fresh garlic cloves induces apoptosis in colon cancer cells via Nrf2. *Nutr. Cancer* **2010**, *62*, 947−957.

(28) Sui, X.; Jin, L.; Huang, X.; Geng, S.; He, C.; Hu, X. p53 signaling and autophagy in cancer: a revolutionary strategy could be developed for cancer treatment. *Autophagy* **2011**, *7*, 565−571.

(29) Soussi, T.; Wiman, K. G. Shaping genetic alterations in human cancer: the p53 mutation paradigm. *Cancer Cell* **2007**, *12*, 303−312.

(30) Ryan, K. M. p53 and autophagy in cancer: guardian of the genome meets guardian of the proteome. *Eur. J. Cancer* **2011**, *47*, 44−50.

(31) Kim, J.; Kundu, M.; Viollet, B.; Guan, K. L. AMPK and mTOR regulate autophagy through direct phosphorylation of Ulk1. *Nat. Cell Biol.* **2011**, *13*, 132−141.
(32) Inoki, K.; Zhu, T.; Guan, K. L. TSC2 mediates cellular energy response to control cell growth and survival. *Cell* **2003**, *115*, 577−590.
(33) Zhou, F.; Yang, Y.; Xing, D. Bcl-2 and Bcl-xL play important roles in the crosstalk between autophagy and apoptosis. *FEBS J.* **2011**, *278*, 403−413.
(34) Mehrpour, M.; Esclatine, A.; Beau, I.; Codogno, P. Overview of macroautophagy regulation in mammalian cells. *Cell Res.* **2010**, *20*, 748−762.
(35) Gargini, R.; Garcia-Escudero, V.; Izquierdo, M. Therapy mediated by mitophagy abrogates tumor progression. *Autophagy* **2011**, *7*, 466−476.
(36) Lisanti, M. P.; Martinez-Outschoorn, U. E.; Chiavarina, B.; Pavlides, S.; Whitaker-Menezes, D.; Tsirigos, A.; Witkiewicz, A.; Lin, Z.; Balliet, R.; Howell, A.; Sotgia, F. Understanding the "lethal" drivers of tumor-stroma co-evolution: emerging role(s) for hypoxia, oxidative stress and autophagy/mitophagy in the tumor micro-environment. *Cancer Biol. Ther.* **2010**, *10*, 537−542.
(37) Kondo, Y.; Kanzawa, T.; Sawaya, R.; Kondo, S. The role of autophagy in cancer development and response to therapy. *Nat. Rev. Cancer* **2005**, *5*, 726−734.